International Journal of Applied Science and Mathematics
Volume 8, Issue 4, ISSN (Online): 2394-2894

Research on Coordinated Control of Active Front Wheel Steering and Direct Yaw Moment

Peilin Shi*, **Liang Zhang, Jianwei Hou, Minglei Liang, Yushuai Zhao and Liaodong Zheng**
School of Transportation and Vehicle Engineering Shandong University of Technology, Shandong, Zibo, Zhangdian, 255049, China.
*Corresponding author email id: ericshi65@163.com

Date of publication (dd/mm/yyyy): 14/07/2021

Abstract **– A coordinated control method of active front steering (AFS) and direct yaw moment (DYC) control system is proposed. Firstly, the expected yaw rate and the expected centroid sideslip angle are solved, then the sliding mode control theory is used to establish the AFS and DYC control systems, the influence of longitudinal speed, front wheel angle and road adhesion coefficient on vehicle stability region is analyzed by β-β˙phase plane. The relationship between the boundary line of the stable region and the road adhesion coefficient is obtained by data fitting. According to the proposed AFS and DYC coordinated control strategy, the coordinated control area is divided, the boundary of coordination region is solved by fuzzy logic method. Finally, the allocation rules of coordination region are formulated. Based on the co-simulation model of Simulink and CarSim, the simulation of double lane change simulation of high and low adhesion coefficient pavement is carried out. The simulation results show that the proposed coordinated control strategy of AFS and DYC is effective, which can improve the operation stability of the vehicle while ensuring the comfort.**

Keywords **– Active Front Wheel Steering, Direct Yaw Moment Control, Coordinated Control, Phase Plane Method, Control Area.**

I. Introduction

With the development of electronic control technology, various chassis control subsystems are installed on the vehicle. Each subsystem controls the corresponding degree of freedom, and there are interference problems between different chassis control subsystems. For example, active front steering (AFS) and direct yaw moment (DYC) control can improve vehicle stability [1]. But the best action area of AFS is the linear area with small lateral acceleration and tire cornering angle [2], and the control has little effect on longitudinal speed and good comfort; The control region of DYC is not limited to the linear region of tire, even in the nonlinear region can obtain good control effect, however, the longitudinal velocity will change when DYC is controlled, and the comfort is poor. Therefore, it is necessary to study the coordinated control of AFS and DYC. The two control systems have complementary advantages to ensure comfort and improve vehicle stability. Many scholars have studied the integrated control of AFS and DYC [3-5], Sang Nan proposed an integrated adaptive control method of AFS and DYC based on Lyapunov theory. The simulation experiments on different adhesion conditions show that the integrated control method can effectively control the lateral dynamic characteristics of vehicles, and the effect is better than that of single control [6]. Liu Li proposed a switching algorithm of vehicle chassis integrated control system based on generalized prediction theory, and realized the switching by adjusting the control weight in real time [7]. Narjes Ahmadian proposes an integrated adaptive coordination technique for active front steering (AFS) and direct yaw moment control (DYC). The main contribution is to present an integrated multi-input multi-output (MIMO) adaptive control method to manage the variations of vehicle mass and tire-road friction coefficient as parameter uncertainties [8]. These chassis integration methods need to establish accurate prediction models, and complex models also bring large amount of calculation. In this paper, the control system of AFS and DYC is designed based on sliding mode variable structure control method. Then the steady state boundary of the vehicle is determined by phase plane method, and the coordinated control area of AFS and DYC is solved by fuzzy logic method. Finally, the allocation rules are formulated to give full play to the control advantages of AFS and DYC.

II. Vehicle Dynamics Model

The 2-DOF linear vehicle model simplifies the vehicle, only retains the lateral and yaw motion, and clearly expresses the relationship between the vehicle yaw rate and the sideslip angle of the centroid and the front wheel angle, which can accurately describe the steering characteristics of the vehicle. So the ideal reference model established in this section is linear two degree of freedom model, the state space equation is as follows :

$$\begin{bmatrix} \dot{\beta} \\ \dot{\gamma} \end{bmatrix} = \begin{bmatrix} a_{11} & a_{12} \\ a_{21} & a_{22} \end{bmatrix} \begin{bmatrix} \beta \\ \gamma \end{bmatrix} + \begin{bmatrix} b_1 \\ b_2 \end{bmatrix} \delta_{\mathrm{f}} \tag{1}$$

Among them, $a_{11} = \frac{k_1+k_2}{mv_x}$, $a_{12} = \frac{ak_1-bk_2}{mv_x^2}$, $a_{21} = \frac{ak_1-bk_2}{I_z}$, $a_{22} = \frac{a^2k_1+b^2k_2}{I_z v_x}$, $b_1 = -\frac{k_1}{mv_x}$, $b_2 = -\frac{ak_1}{I_z}$.

In the formula, β is sideslip angle. $I_z$is yaw inertia.$\gamma$is yaw rate. δ_f is the front wheel angle.aandb are the distances from the front and rear axes to the centroid. mis vehicle quality. v_x is the longitudinal speed of the vehicle. k_1 andk_2 are the lateral stiffness of the front and rear wheels.

Let $[\dot{\beta} \quad \dot{\gamma}]^T = 0$, the yaw rate and sideslip angle of mass center under steady state conditions can be calculated as :

$$\gamma_d = \frac{v_x/L}{1+Kv_x^2}\delta_{\mathrm{f}} \tag{2}$$

$$\beta_{\mathrm{d}} = \frac{b+mav_x^2/(k_2L)}{L(1+Kv_x^2)}\delta_{\mathrm{f}} \tag{3}$$

In the formula, γ_d and β_d are the yaw rate and sideslip angle under steady state conditions, respectively; $K = \frac{m}{(a+b)^2}\left(\frac{a}{k_2} - \frac{b}{k_1}\right)$ is the vehicle stability factor ; L is the vehicle axle distance.

At the same time, considering the limit of road adhesion conditions on vehicle yaw rate and sideslip angle, the upper limit is [9] :

$$|\gamma_{\mathrm{dmax}}| \le \left|\frac{\mu g}{v_x}\right| \tag{4}$$

$$\beta_{\mathrm{dmax}} \le \arctan\,(0.02\mu g) \tag{5}$$

Therefore, the final determined expected yaw rate and expected centroid sideslip angle are :

$$\gamma_{\mathrm{d}} = \min\left\{\left|\frac{v_x/L}{1+Kv_x^2}\delta_{\mathrm{f}}\right|, \left|\frac{\mu g}{v_x}\right|\right\}\mathrm{sgn}(\delta_{\mathrm{f}}) \tag{6}$$

$$\beta_{\mathrm{d}} = \left\{\left|\frac{b+mav_x^2/(k_2L)}{L(1+Kv_x^2)}\delta_{\mathrm{f}}\right|, |\arctan\,(0.02\mu g)|\right\}\mathrm{sgn}(\delta_{\mathrm{f}}) \tag{7}$$

III. AFS Control System and DYC System

The actual vehicle system has many uncertainties and complexity, including the change of vehicle parameters and the interference of external environment. It is difficult to establish an accurate mathematical model, which leads to some control methods that need to rely on accurate models to act on the vehicle system, and cannot play the desired effect. However, due to its strong robustness, sliding mode control can achieve the desired control effect under the influence of some uncertain factors, which can be used to design AFS and DYC control systems [10].

The active front wheel steering selects the difference between the actual yaw rate and the ideal yaw rate as the control error of the system. The direct yaw moment control system selects the difference between the actual yaw rate and the ideal yaw rate, the actual centroid sideslip angle and the ideal centroid sideslip angle as the control error of the system. The expression is :

$$e_{\text{afs}} = \gamma - \gamma_{\text{d}} \tag{8}$$

$$e_{\text{dyc}} = (\gamma - \gamma_{\text{d}}) + \rho(\beta - \beta_{\text{d}}) \tag{9}$$

In the formula, e_{afs} and e_{dyc} are the control errors of AFS control system and DYC control system respectively.

The selected switching function is :

$$s = e + \lambda \int_0^t e(\tau)\, d \tag{10}$$

In the formula, λ is a positive weighting coefficient, which is proportional to the convergence speed of sliding mode control. $\lambda \int_0^t e(\tau)\, d\tau$is mainly used to limit steady-state error.

Derivation of (10) can be obtained :

$$\dot{s}_{\text{afs}} = \dot{e}_{\text{afs}} + \lambda_{\text{afs}} e_{\text{afs}} = \dot{\gamma} - \dot{\gamma}_{\text{d}} + \lambda_{\text{afs}}(\gamma - \gamma_{\text{d}}) \tag{11}$$

$$\dot{s}_{\text{dyc}} = \dot{e}_{\text{dyc}} + \lambda_{\text{dyc}} e_{\text{dyc}} = \dot{\gamma} - \dot{\gamma}_{\text{d}} + \rho(\dot{\beta} - \dot{\beta}_{\text{d}}) + \lambda_{\text{dyc}}(\gamma - \gamma_{\text{d}}) + \rho\lambda_{\text{dyc}}(\beta - \beta_{\text{d}}) \tag{12}$$

In AFS control system, the expression of $\dot{\gamma}$ is :

$$\dot{\gamma} = \text{a}_{21}\beta + \text{a}_{22}\gamma + \text{b}_2\delta_{\text{f}} \tag{13}$$

Substituting Eq. (13) into Eq. (11), the AFS control law equation under sliding mode is obtained:

$$\dot{s}_{\text{afs}} = \text{a}_{21}\beta + \text{a}_{22}\gamma + \text{b}_2\delta_{\text{f}} - \dot{\gamma}_{\text{d}} + \lambda_{\text{afs}}(\gamma - \gamma_{\text{d}}) \tag{14}$$

Let s $\dot{s}_{\text{afs}} = 0$ obtain the equivalent control input :

$$\delta_{\text{afs}} = \frac{1}{\text{b}_2}[-\text{a}_{21}\beta - \text{a}_{22}\gamma + \dot{\gamma}_{\text{d}} - \lambda_{\text{afs}}(\gamma - \gamma_{\text{d}})] \tag{15}$$

δ_{afs} is the additional front wheel angle that the AFS control system needs to provide.

In the DYC control system, the design of the control system needs to establish a linear two-degree-of-freedom model considering the additional yaw moment M_z. The state space equation is as follows :

$$\begin{bmatrix} \dot{\beta} \\ \dot{\gamma} \end{bmatrix} = \begin{bmatrix} a_{11} & a_{12} \\ a_{21} & a_{22} \end{bmatrix} \begin{bmatrix} \beta \\ \gamma \end{bmatrix} + \begin{bmatrix} b_1 \\ b_2 \end{bmatrix} \delta_{\text{f}} + \begin{bmatrix} c_1 \\ c_2 \end{bmatrix} M_z \tag{16}$$

In the formula, $\text{c}_1 = 0$, $\text{c}_2 = \frac{1}{\text{I}_\text{z}}$.

From formula (16) :

$$\dot{\beta} = a_{11}\beta + a_{12}\gamma + b_1\delta_f + c_1 M_z \tag{17}$$

$$\dot{\gamma} = a_{21}\beta + a_{22}\gamma + b_2\delta_f + c_2 M_z \tag{18}$$

Substituting Eqs. (17) and (18) into Eq. (12), the DYC control law equation under sliding mode is obtained:

$$\dot{s}_{dyc} = a_{21}\beta + a_{22}\gamma + b_2\delta_f + c_2 M_z - \dot{\gamma}_d + \rho(a_{11}\beta + a_{12}\gamma + b_1\delta_f + c_1 M_z - \beta_d) + \lambda_{dyc}(\gamma - \gamma_d) + \rho\lambda_{dyc}(\beta - \beta_d) \tag{19}$$

Let $\dot{s}_{dyc} = 0$ to obtain the equivalent control input :

$$M_z = -\frac{1}{c_2}\left[a_{21}\beta + a_{22}\gamma + b_2\delta_f - \dot{\gamma}_d + \rho(a_{11}\beta + a_{12}\gamma + b_1\delta_f - \beta_d) + \lambda_{dyc}(\gamma - \gamma_d) + \rho\lambda_{dyc}(\beta - \beta_d)\right] \tag{20}$$

M_z is the additional yaw moment. The braking mode in this paper is single wheel braking. According to the definition of vehicle coordinate system, the braking wheel corresponding to different driving states is shown in table 1 when the vehicle moves forward from left to right.

Table 1. Direct yaw moment control strategy.

γ	$\gamma - \gamma_d$	**Motoring Condition**	**Brake Wheel**
+	+	Oversteering	Right-front wheel
+	0	Neutral steer	None
+	-	Understeering	Left-front wheel
-	+	Understeering	Right-rear wheel
-	0	Neutral steer	None
-	-	Oversteering	Left-rear wheel

It is necessary to consider the limit value of braking force when the tire has lateral force. It can be obtained from the friction ellipse :

$$F_{xi}^2 + F_{yi}^2 \le \mu_i^2 F_{zi}^2 \tag{21}$$

In the formula, F_{xi}, F_{yi} and F_{zi} are the longitudinal force, lateral force and vertical load of the tire, respectively, and μ_i is the longitudinal rolling friction coefficient.

Therefore, when allocating braking force, the following conditions should be satisfied:

$$0 \le F_{xi} \le \sqrt{\mu_i^2 F_{zi}^2 - F_{yi}^2} \tag{22}$$

When braking, the longitudinal force is negative, the yaw moment generated when the vehicle turns left is positive, and the right is negative. The calculation formula of the yaw moment generated by the four wheels is:

$$M_{fl} = F_{x1}\left(a\sin\delta_f - \frac{B_f}{2}\cos\delta_f\right) \tag{23}$$

$$M_{fr} = F_{x2}\left(a\sin\delta_f + \frac{B_f}{2}\cos\delta_f\right) \tag{24}$$

$$M_{rl} = -F_{x3}\frac{B_r}{2} \tag{25}$$

$$M_{\mathrm{rr}} = F_{x4}\frac{B_{\mathrm{r}}}{2} \tag{26}$$

In the formula, M_{fl}, M_{fr}, M_{rl} and M_{rr} correspond to the yaw moment of the left front wheel, the right front wheel, the left rear wheel and the right rear wheel, and B_f and B_r are the wheel spacing of the front and rear axles.

IV. Coordinated Control Strategy

A. *Division of Stable Regions*

At present, the main method for vehicle stability region division is the phase plane method of state parameters [11]. The phase plane method of state parameters is divided into two kinds: sideslip angle - yaw velocity ($\beta-\gamma$) and sideslip angle - sideslip angle velocity ($\beta-\dot{\beta}$), Tian Chen [10] proposed that on low adhesion road, the change rate of sideslip angle of centroid is large, and the vehicle is prone to sideslip. Since the $\beta-\gamma$ phase plane ignores the influence of the centroid sideslip angular velocity, the stable region cannot be accurately divided. The $\beta-\dot{\beta}$ phase plane can evaluate the state of vehicles on both high and low adhesion roads, so in this paper, the $\beta-\dot{\beta}$ phase plane is selected to divide the stable region.

The division of the stable region in the $\beta-\dot{\beta}$ phase plane is mainly based on the double straight line method, which adopts two straight lines symmetric origin are adopted, as shown in Figure 1. In the figure, the straight lines AB and CD are the two boundary lines of the plane stability region of $\beta-\dot{\beta}$ phase divided by the double straight line method. The region between the straight lines AB and CD is the stable region, which is expressed as:

$$\left|\dot{\beta} + B_1\beta\right| \le B_2 \tag{27}$$

In the formula, B_1 and B_2 are the slope and intercept of the boundary line respectively.

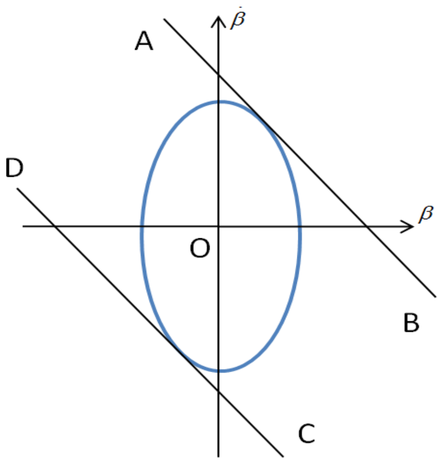

Fig. 1. Double line method.

In this paper, the influence of longitudinal speed, front wheel angle and road adhesion coefficient on vehicle stability area is analyzed by controlling factors.

The road adhesion coefficient is 0.9 and there is no front wheel angle. The phase diagram of 20km/h, 60km/h and 120km/h is drawn, as shown in Figure 2.

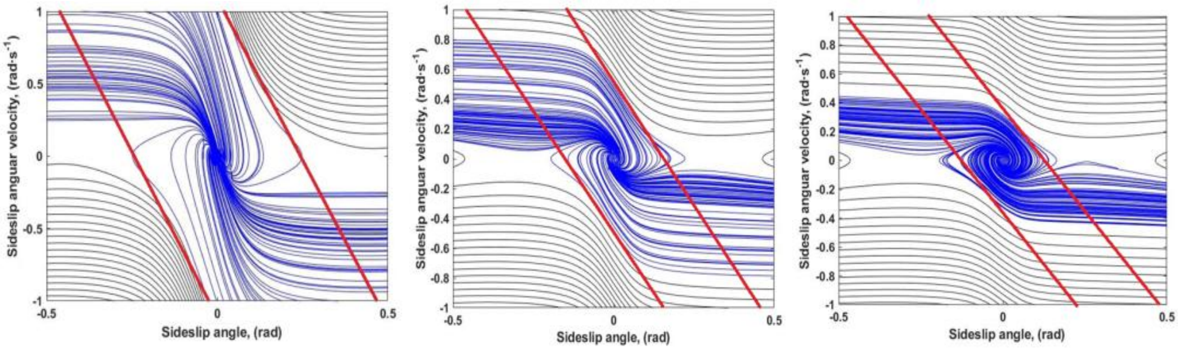

(a) 20km/h (b) 60km/h (c) 120km/h

Fig. 2. Phase plane stability region at different longitudinal speeds.

When the vehicle speed is 60 km/h and the road adhesion coefficient is 0.9, the phase plane diagram of the front wheel angle of 2°,6° and 10° is drawn, as shown in figure 3.

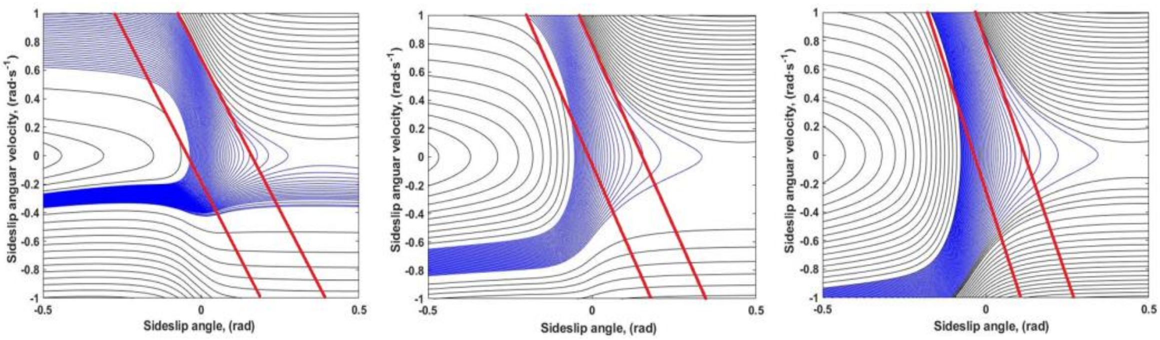

(a) 2° (b) 6° (c) 10°

Fig. 3. Phase plane stability region at different front wheel angles.

When the vehicle speed is 60 km/h and there is no front wheel angle, the phase plane diagram of the road adhesion coefficient is 0.1, 0.5 and 1, as shown in figure 4.

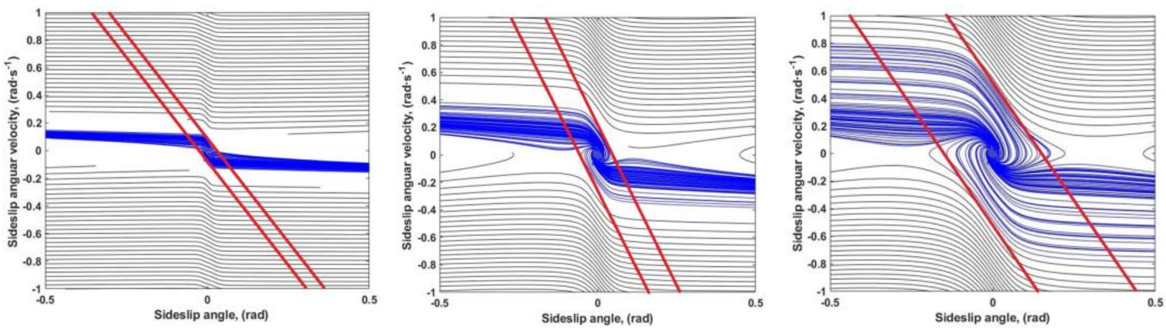

(a) $\mu = 0.1$ (b) $\mu = 0.5$ (c) $\mu = 1$

Fig. 4. Phase plane stability region under different road adhesion coefficients.

From figure 2, it can be seen that the stability region of $\beta - \dot{\beta}$ phase plane graph is larger at low speed, and the stability region of vehicle phase plane graph shows a decreasing trend at high speed, when the vehicle speed exceeds a certain value, the change is very small, almost unchanged. In Figure 3, when the front wheel angle gradually increases, the stable region of the $\beta - \dot{\beta}$ phase plane diagram changes little. In Figure 4, the change of road adhesion coefficient has a great influence on the stable region of β-β· phase plane graph. When the road

International Journal of Applied Science and Mathematics
Volume 8, Issue 4, ISSN (Online): 2394-2894

adhesion coefficient increases from 0.1 to 1, the range of stable region gradually becomes larger. When the road adhesion coefficient is 0.1, the stable region is very small, it shows that the vehicle is easily unstable at this time, which is also in line with the actual operation characteristics of the vehicle. Therefore, this paper obtains the corresponding parameters by drawing the $\beta - \dot{\beta}$ phase plane under different road adhesion coefficients, as shown in Table 2. The relationship between the slope and intercept of the boundary line and the road adhesion coefficient is obtained by fitting the data in the table.

Table 2. Stable region parameters of different road adhesion coefficients.

μ	B_1	B_2	Width of Stable Region
0.1	3.2632	0.014	0.02658
0.2	3.5088	0.027	0.05233
0.3	3.7126	0.038	0.07578
0.4	5.0270	0.061	0.1189
0.5	5.3149	0.074	0.1422
0.6	5.5856	0.081	0.1577
0.7	6.0563	0.1093	0.1991
0.8	6.8932	0.1256	0.2428
0.9	7.6254	0.1415	0.2786
1	7.9623	0.1626	0.3288

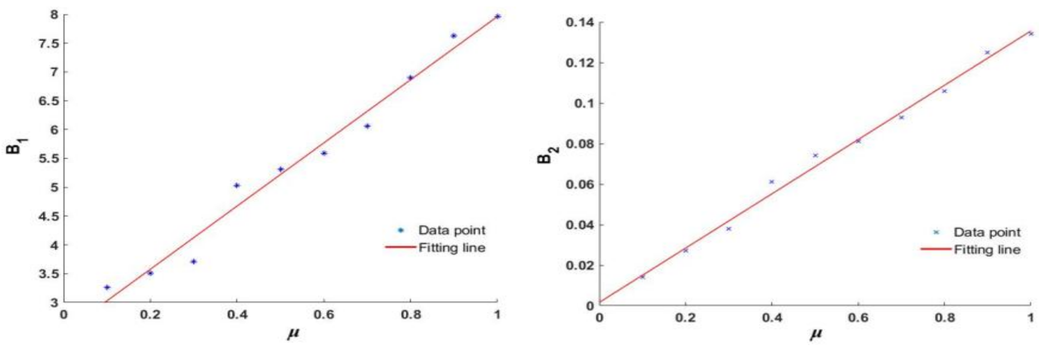

(a) B_1 fitting line.

(b) B_2 fitting line.

Fig. 5. Fitting of slope and intercept.

The fitting relationship between slope B_1 and road adhesion coefficient is :

$$B_1 = 5.477\mu + 2.4826 \tag{28}$$

The fitting relationship between intercept B_2 and road adhesion coefficient is:

$$B_2 = 0.134\mu + 0.00167 \tag{29}$$

B. *Coordinated Control Region Division*

The coordinated control of this paper includes three stages: single AFS control, coordinated control of AFS and DYC, single DYC control. The corresponding phase plane must be divided into three control areas: AFS control area, coordinated control area, DYC control area.

According to the characteristic analysis of the active front steering system, the active front steering system works mainly in the vehicle stability region, so when dividing the region, the boundary of the stability region is generally regarded as the boundary of the active front steering control, the relationship is :

$$|\dot{\beta} + B_1\beta| = B_2 \tag{30}$$

Outside the boundary, direct yaw moment control is required, the relationship is :

$$|\dot{\beta} + B_1\beta| > B_2 \tag{31}$$

The fitting equations (28) and (29) obtained from Section 3.1 can determine the AFS control boundary and the DYC control boundary under different road adhesion coefficients. However, by analyzing the stability regions under different longitudinal speeds and front wheel angles, it is found that the longitudinal speed and front wheel angle have certain influence on the stability region. Therefore, the role of longitudinal speed and front wheel angle should be considered in dividing the coordinated control region. When the vehicle speed is small, the phase plane boundary determined by the road adhesion coefficient can appropriately increase outward, and when the vehicle speed is large, the phase plane boundary can appropriately shrink inward. Similarly, when the front wheel angle is small, the boundary can be appropriately increased outward, and when the front wheel angle is large, the boundary needs to be appropriately reduced. That is, an elastic region is added at the boundary line of phase plane determined by the road adhesion coefficient as the coordination region.

Therefore, this paper determines the three control areas, the corresponding range formula is as follows:

(1) AFS control region :

$$|\dot{\beta} + B_1\beta| \le q_1 B_2 \tag{32}$$

(2) Coordinated control region :

$$q_1 B_2 < |\dot{\beta} + B_1\beta| < q_2 B_2 \tag{33}$$

(3) DYC control region :

$$q_2 B_2 \le |\dot{\beta} + B_1\beta| \tag{34}$$

In the formula, $q_1$andq_2 are weighted coefficients, $0 < q_1 \le 1$,$q_2 \ge 1$. The divided area is shown in Figure 6.

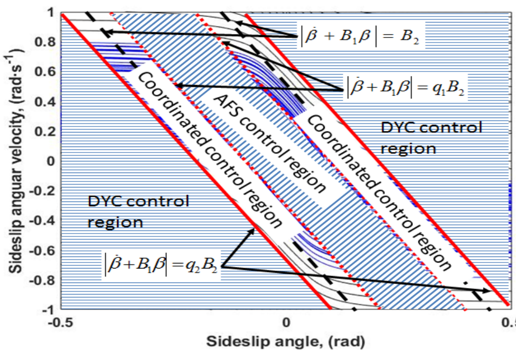

Fig. 6. Division of Coordinated Control Areas.

In this paper, fuzzy logic control method is selected to solve the weighted coefficients q_1 and q_2. In the above analysis, it is known that the boundary of the stable region needs to be narrowed when the vehicle speed increases or the front wheel angle increases. Therefore, the longitudinal vehicle speed and the front wheel angle are selected as the input and the output is q_1 and q_2. Setting longitudinal speed has 5 fuzzy subsets and front wheel angle has 9 fuzzy subsets. The maximum vehicle speed is 120km/h and the maximum front wheel angle is 39 degrees, so the physical domain of longitudinal speed is (0, 120). The physical domain of the front wheel angle is (−39, 39). Finally, the domain after quantifying the longitudinal speed and front wheel angle is taken as:

Longitudinal speed :{0, 1, 2, 3, 4, 5, 6, 7, 8, 9, 10, 11, 12}; Front wheel angle: {-8, -7, -6, -5, -4, -3, -2, -1, 0, 1, 2, 3, 4, 5, 6, 7, 8}, The input membership function is shown in Figure 7.

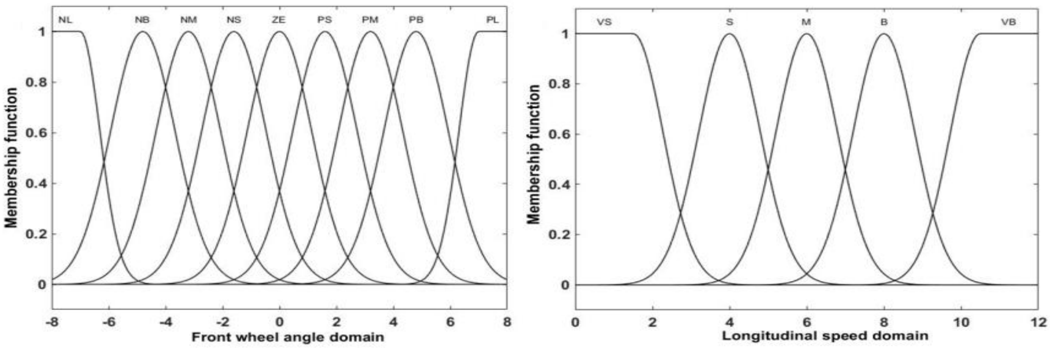

(a) Front wheel angle (b) Longitudinal speed

Fig. 7. Input membership function.

Set the weighted coefficient q_1 to (0.5, 1) and the weighted coefficient q_2 to (1, 1.5). The output membership function is shown in Figure 8.

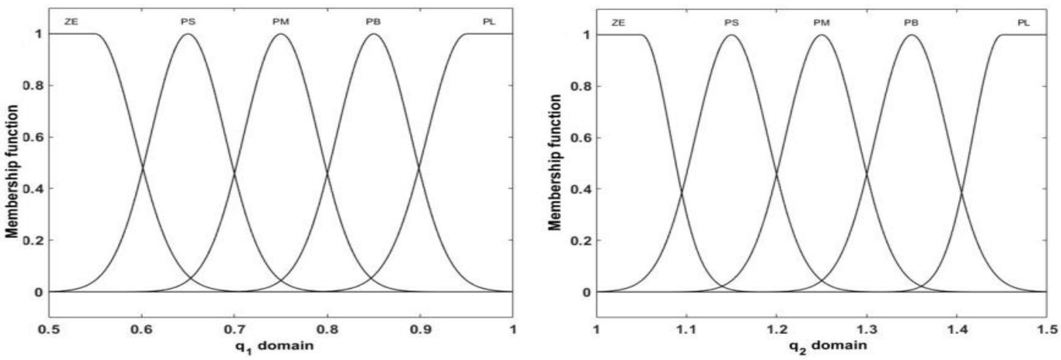

(a) Weighted coefficient q_1 (b) Weighted coefficient q_2

Fig. 8. Input membership function.

Make fuzzy control rules according to actual situation and experience, and remove unreasonable situation. After many simulations, the fuzzy control rules determined in this paper are shown in Table 3.

Table 3. Fuzzy control rules.

q_1, q_2 / v_x / δ_f	VS	S	M	B	VB
NL	PL,PM	PB,PS	PM,ZE	PS,ZE	ZE,ZE
NB	PL,PM	PL,PM	PB,PS	PM,ZE	PS,ZE

q_1, q_2 \ v_x / δ_f	**VS**	**S**	**M**	**B**	**VB**
NM	PL, PB	PL, PB	PL, PM	PB, PS	PM, ZE
NS	PL, PL	PL, PL	PL, PB	PB, PM	PM, PS
ZE	PL, PL	PL, PL	PL, PL	PL, PB	PB, PM
PS	PL, PL	PL, PL	PL, PB	PB, PM	PM, PS
PM	PL, PB	PL, PB	PL, PM	PB, PS	PM, ZE
PB	PL, PM	PL, PM	PB, PS	PM, ZE	PS, ZE
PL	PL, PM	PB, PS	PM, ZE	PS, ZE	ZE, ZE

After determining the coordinated control area, it is also necessary to reasonably design the switching rules of AFS and DYC control, and allocate the control time and strength of active front wheel steering and direct yaw moment. Therefore, the coordination parameters q_s and q_m of AFS control and DYC control are designed in the coordination region in this paper. When AFS works alone, $q_s = 1$, $q_m = 0$. When DYC works alone, $q_s = 0$, $q_m = 1$. In the coordination of the two systems, the S-type membership function is selected to solve the coordination parameters. The expression for calculating the coordination parameter q_s of active front wheel steering is as follows :

$$q_s(x) = \begin{cases} 1 & x \le i_a \\ 1 - i_m\left(\frac{x-i_a}{i_b-i_a}\right)^2 & i_a < x \le \frac{i_b+i_a}{2} \\ i_n\left(\frac{x-i_b}{i_b-i_a}\right)^2 & \frac{i_b+i_a}{2} < x < i_b \\ 0 & x \ge i_b \end{cases} \tag{35}$$

In the formula, $i_a = q_1 B_2$, $i_b = q_2 B_2$, i_m and i_n are the adjustment parameters, and the coordination parameter q_m of the direct yaw moment is expressed as follows:

$$q_m = 1 - q_s \tag{36}$$

V. Simulation Analysis

The co-simulation model of Simulink and CarSim is established, and the main parameters of the vehicle [12] are shown in Table 4.

Table 4. Main vehicle parameters.

Name	**Value**	**Name**	**Value**
Complete vehicle quality m/kg	1110	Distance from front axle to centroida/m	1.04
Yaw inertialI_z/(kg·m2)	1343.1	Distance from rear axle to centroid b/m	1.56
Distance between front wheelsB_f/m	1.48	Front wheel lateral stiffnessk_1/(N·rad-1)	-47904
Distance between rear wheelsB_r/m	1.485	Rear wheel lateral stiffness k_2/(N·rad-1)	-56366

The initial vehicle speed is 70 km/h, and the double lane-shifting simulation is carried out on the roads with the adhesion coefficients of 0.85 and 0.3, respectively.

A. *High Adhesion Road*

The operation results of the simulation model are shown in Figure 9.

From the simulation results shown in Figure 9a) and Figure 9b), single AFS control, single DYC control and coordinated control system can well control the yaw rate and the sideslip angle of the centroid of the vehicle under the condition of double lane change. The yaw rate and sideslip angle under DYC control are the smallest, the control effect of coordinated control is close to that of single AFS control. As can be seen from the longitudinal speed in Figure 9c), under the control of single DYC, the reduction of vehicle speed is the largest, and the interference of single AFS control on vehicle speed is the smallest, and the vehicle speed is slightly higher than the longitudinal speed without control, and the coordinated control is between the two. Figure 9d) is the driving track of the vehicle. It can be seen that the three control methods all reduce the lateral displacement of the vehicle. The lateral displacement under the coordinated control is the smallest, and the control effect is slightly better than that under the single DYC control. The lateral displacement after the single AFS control is the largest.

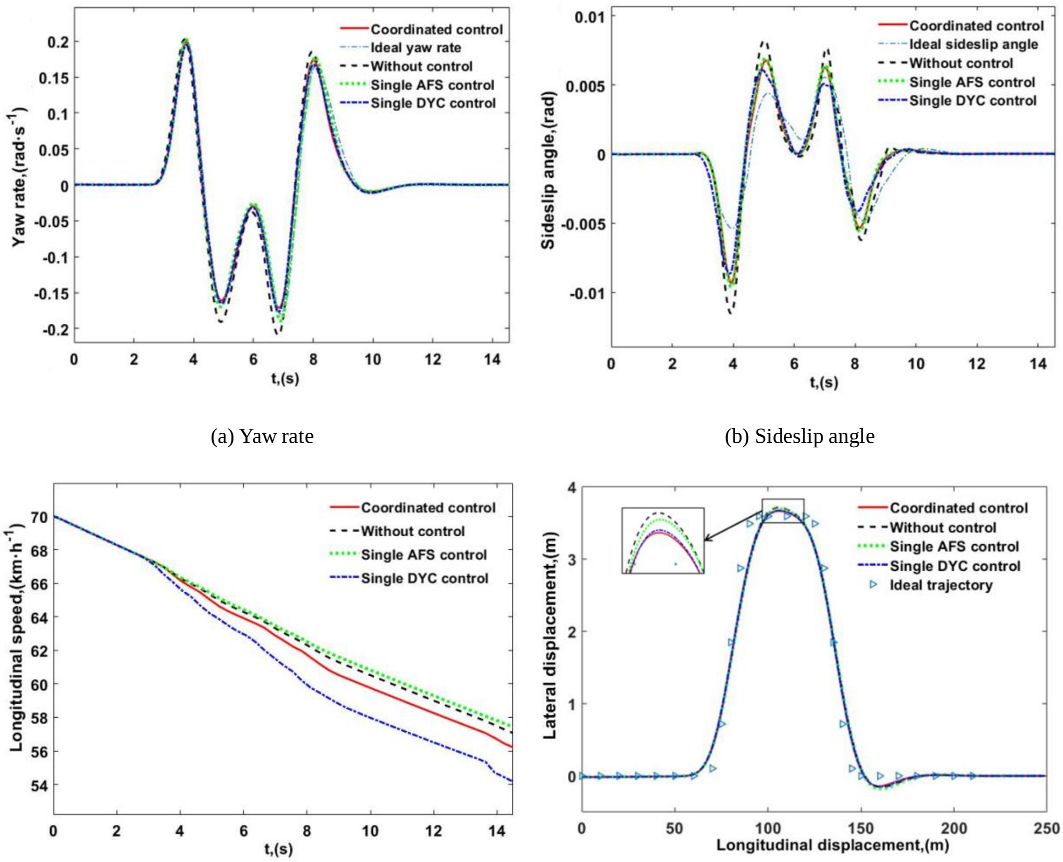

(a) Yaw rate (b) Sideslip angle

(c) Longitudinal speed (D) Driving track

Fig. 9. Simulation results of high adhesion road.

B. *Low Adhesion Road*

The operation results of the simulation model are shown in Figure 10.

It can be seen from Figure 10a) and Figure 10b) that when the double lane change operation is carried out on the low adhesion pavement, the vehicle without control and the vehicle with single AFS control have serious sideslip. The yaw and sideslip of the vehicle are very serious and have completely lost control. Vehicles under single DYC control and coordinated control can maintain a stable state, the yaw rate under the control of DYC alone can still follow the ideal value, and the sideslip angle of the centroid is also controlled near the ideal value. The yaw rate under coordinated control fluctuates around the ideal value, which is caused by the switching between steering and braking. It can be seen from Figure 10a) that the yaw rate under DYC control has obvious buffeting phenomenon. Figure 10c) shows that the longitudinal speed reduction under coordinated control is the lowest and the interference to the driver is the smallest. Figure 10d) shows that the vehicle lateral displacement under coordinated control is the smallest and the ideal path tracking effect is the best.

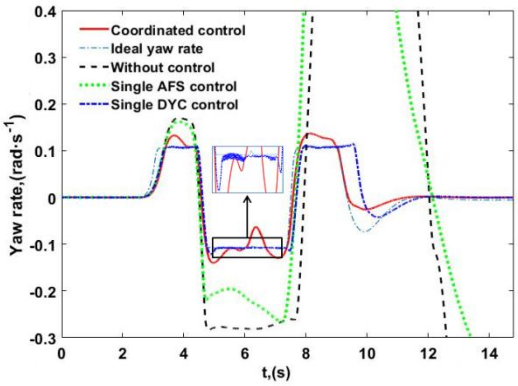

(a) Yaw rate

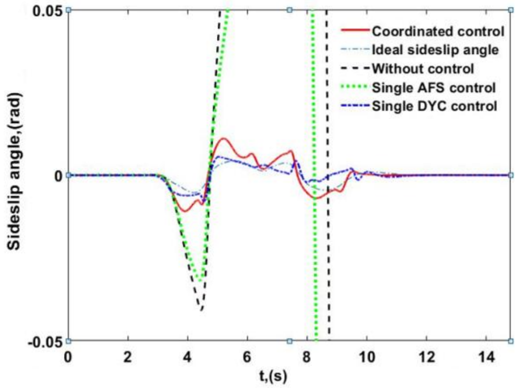

(b) Sideslip angle

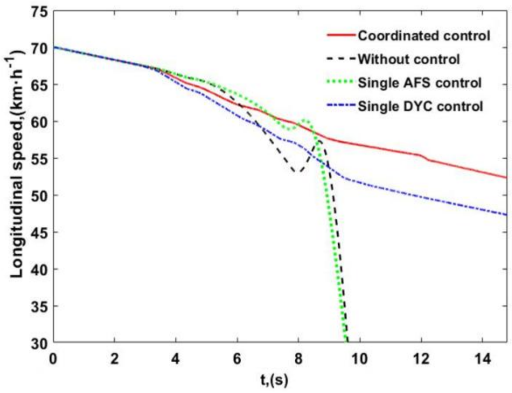

(c) Longitudinal speed

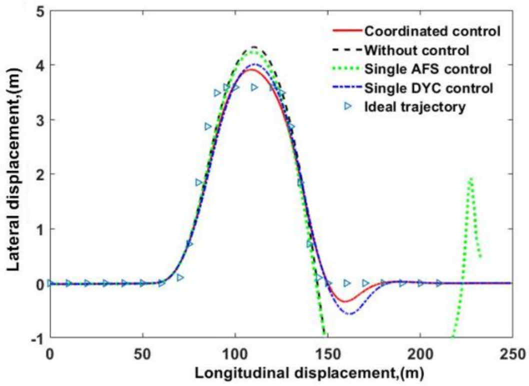

(d) Driving track

Fig. 10. Simulation results of low adhesion road.

VI. Conclusion

In this paper, the expected yaw rate and centroid sideslip angle are solved, and the limitation of road adhesion coefficient on the expected value is considered. The sliding mode control theory is used to design AFS control system and DYC control system. The control variables of AFS control system are expected yaw rate, and the control variables of DYC control system are expected yaw rate and sideslip angle. The phase plane method is used to divide the stable region of the vehicle. By fitting the boundary data of the stable region determined by the road adhesion coefficient, the relationship between the slope and intercept of the boundary line and the road adhesion coefficient is obtained. Three areas of coordinated control are divided, namely AFS control area, coordinated control area and DYC control area. The boundary of coordination region is solved by fuzzy logic method, and the allocation rules are formulated. The joint simulation model of CarSim and MATLAB/Simulink is established to simulate the double lane-changing conditions of high and low adhesion coefficient roads. The results show that, in the case of high adhesion road, single AFS control and single DYC control can effectively improve the stability of the vehicle, but the comfort of DYC control is poor. The coordinated control system is mainly comfortable, and the control effect of comfort and stability is obtained. On the low adhesion road, the single AFS control system almost lost its function, and the single DYC control can effectively improve the stability. The coordinated control system is mainly based on stability. The control effect is better than that of the single DYC control, and the comfort is better.

REFERENCES

[1] Zhi-Jun Fu, Bin Li. Adaptive optimal control for integrated active front steering and direct yaw moment based on approximate dynamic programming [J]. Int. J. of Vehicle Systems Modelling and Testing, 12(1/2), 2017.
[2] Sang Nan, Liu Runqiao, ZhaoWanzhong. Coordinated control of active front wheel steering and direct yaw moment for vehicles. Journal of Nanjing University of Technology, 42(06): 655-661., 2018.
[3] Chen Wuwei, Liang Xiutian, Wang Qidong, et al. Extension coordinated control of four wheel independent drive electric vehicles by AFS and DYC[J]. Control Engineering Practice, 101(C), 2020.
[4] Meng Qinghua, Zhao Tingting, Qian Chunjiang, et al. Integrated stability control of AFS and DYC for electric vehicle based on non-smooth control[J]. International Journal of Systems Science, Vol. 49, Issue 7, pp. 1518-1528, 2018.
[5] Wei Jianwei, Zhao Wanzhong. Combined Control Strategy of AFS and DYC for New Electric Wheel Steering System [J]. Mechanical Science and Technology, 37(01):108-114, 2018.
[6] Sang Nan, Wei Minxiang. Adaptive control of vehicle active front wheel steering and direct yaw moment [J]. Journal of Transportation Engineering, 16(03):91-99, 2016.
[7] Liu Li, Luo Yugong, Jiang Qingyun, et al. Integrated control of AFS/DYC chassis based on generalized prediction theory [J]. Automotive Engineering, 33(01): 52-55+ 46, 2011.
[8] Narjes Ahmadian, Alireza Khosravi, Pouria Sarhadi. Integrated model reference adaptive control to coordinate active front steering and direct yaw moment control[J].ISA Transactions, Vol. 106, pp.85-96, 2020.
[9] Chen Wuwei, Liu Xiangyu, Huang He, et al. Dynamic Boundary Control of Sideslip Angle for Vehicle Stability Control Considering Pavement Influence. Chinese Journal of Mechanical Engineering, 48(14):112-118, 2012.
[10] Tian Chen. Coordinated Control of AFS and DYC Based on Kalman Filter. Hunan university, 2017.
[11] Li Jing, Wang Zihan, Wang Xuanfeng. Stability analysis of braking direction based on phase plane method. Automotive Engineering, 36(08): 974-979, 2014.
[12] Feng Xiaozhi, Shi Peilin, Cao Fan, et al. Design and research on ideal transmission ratio of steer-by-wire vehicle based on CarSim. Journal of Guangxi University (Natural Science Edition), 43(06): 2122-2132, 2018.

AUTHOR'S PROFILE

First Author
Peilin Shi, Doctor of Engineering, Male, Associate professor. School of Transportation and Vehicle Engineering, Shandong University of Technology, Shandong, Zibo, Zhangdian, 255049, China (First author). You can contact with Peilin Shi, Thank you! email id: ericshi65@163.com

Second Author
Liang Zhang, Master in reading, Male, School of Transportation and Vehicle Engineering, Shandong University of Technology, Shandong, Zibo, Zhangdian, 255049, China. You can contact with the Liang Zhang, Thank you!
email id: 1358224770@qq.com

Third Author
Jianwei Hou, Master in reading, Male, School of Transportation and Vehicle Engineering, Shandong University of Technology, Shandong, Zibo, Zhangdian, 255049, China.

Fourth Author
Minglei Liang, Master in reading, Male, School of Transportation and Vehicle Engineering, Shandong University of Technology, Shandong, Zibo, Zhangdian, 255049, China.

Fifth Author
Yushuai Zhao, Master in reading, Male, School of Transportation and Vehicle Engineering, Shandong University of Technology, Shandong, Zibo, Zhangdian, 255049, China.

Sixth Author
Liaodong Zheng, Master in reading, Male, School of Transportation and Vehicle Engineering, Shandong University of Technology, Shandong, Zibo, Zhangdian, 255049, China.